Therapeutic Discovery

Molecular Cancer Therapeutics

Human Monoclonal Antibody Fragments Binding to Insulin-like Growth Factors I and II with Picomolar Affinity

Qi Zhao, Yang Feng, Zhongyu Zhu, and Dimiter S. Dimitrov

Abstract

The type 1 insulin-like growth factor receptor (IGF1R) and its ligands (IGF-I and IGF-II) have been implicated in a variety of physiologic processes and in diseases such as cancer. In addition to IGF1R, IGF-II also activates the insulin receptor (IR) isoform A, and therefore, antibodies against IGF-II can inhibit cell proliferation mediated by the signaling through both IGF1R and IR triggered by IGF-II. We identified a new human monoclonal antibody (mAb), m708.2, which is bound to IGF-I and IGF-II but not to insulin. m708.2 potently inhibited signal transduction mediated by the interaction of IGF-I or IGF-II with the IGF1R and IGF-II with the IR. It also inhibited the growth of the breast cancer cell line MCF-7. An affinity-matured derivative of m708.2, m708.5, bound to IGF-I with equilibrium dissociation constant, $K_D = 200$ pmol/L and to IGF-II with $K_D = 60$ pmol/L. m708.5 inhibited signal transduction mediated by IGF-I and IGF-II and cancer cell growth more potently than m708.2. These results suggest that m708.5 could have potential as a candidate therapeutic for cancers driven by the IGF-I and IGF-II interactions with IGF1R and IR. *Mol Cancer Ther; 10(9); 1677–85. ©2011 AACR.*

Introduction

The type 1 insulin-like growth factor receptor (IGF1R) and its ligands (IGF-I and IGF-II) have been implicated in a variety of physiologic processes and in pathologic conditions such as cancer (1–4). Although the role of the IGF system in cancer has been recognized many years ago, it is not until recent years that the system's components have been targeted and shown to affect cell transformation, proliferation, survival, motility, and migration in tissue cultures and in mouse models of cancers (5–7). The IGF1R shares a similar tetrameric $\alpha 2\beta 2$ structure with insulin receptor (IR). The IGF-mediated signaling is initiated by the binding of IGF-I and IGF-II to their receptor IGF1R, which induces conformational changes in the transmembrane domain of the β subunit. The conformational changes further lead to transphosphorylation of the kinase domain in the 2 β chains (8). The phosphorylated and fully activated IGF1R recruits adaptor proteins such as insulin receptor substrate (IRS) 1, IRS2, and Src-homology collagen (SHC; ref. 9). The phosphorylation of IRS1 regulates the activity of phosphoinositide 3-kinase and protein kinase B (also known as Akt) and triggers the activation of some transcription factors that control the expression of many genes that are important for cell proliferation and growth (3). Numerous studies show that IGF1R is expressed in a broad panel of tumors, suggesting that inhibition of IGF1R signaling may have both proapoptotic and antiproliferative consequences (10). Thus, it seems that the modulation of the activity of the IGF system could add to the arsenal of anticancer therapeutic approaches (11). Different strategies aimed at targeting the IGF system have been investigated including small molecule tyrosine kinase inhibitors, antisense technologies (12), monoclonal antibodies (mAbs) targeting the IGF1R (10, 13, 14), IGF-I (15), and IGF-II (11, 16). They inhibit the kinase activity or disrupt the interaction of IGF1R with its ligands IGF-I and IGF-II, and downregulate the levels of IGF1R.

MAbs have been highly successful as cancer therapeutics. Great progress in clinical and preclinical stages has been made in developing antibodies aimed at targeting IGF system components (17). During the past several years, a number of mAbs against the IGF1R have been identified with cancer cell growth inhibitory activity (10, 13, 18, 19). However, the IGF1R is not very significantly overexpressed in tumors and the mAbs could bind to normal cells expressing the receptor with possible toxic effects. Antibodies against the ligands IGF-I and IGF-II that inhibit the interaction with IGF1R may not have these undesirable effects. Most anti-IGF1R antibodies do not inhibit IGF1R–IR hybrid receptor. IGF-II-mediated signaling through the hybrid receptor could escape the blockage by IGF1R antibodies. In addition, another consideration is that binding to the ligands, which is not cell associated but is diffusible, may not require significant

Authors' Affiliation: Protein Interactions Group, Center for Cancer Research Nanobiology Program, National Cancer Institute-Frederick, NIH, Frederick, Maryland

Note: Supplementary material for this article is available at Molecular Cancer Therapeutics Online (http://mct.aacrjournals.org/).

Corresponding Author: Dimiter S. Dimitrov, Protein Interactions Group, National Cancer Institute-Frederick, NIH, Bldg 469, Rm 150B, Frederick, MD 21702. Phone: 301-846-1352; Fax: 301-846-5598; E-mail: dimiter.dimitrov@nih.gov

doi: 10.1158/1535-7163.MCT-11-0281

penetration into solid tumors, thus avoiding problems associated with penetration (11). A rat monoclonal antibody KM1468, which is cross-reactive to human IGF-I and IGF-II, could suppress the development of new bone tumors and the progression of established tumors (20, 21). KM1468 inhibits tumor growth and increases survival in a mouse model of hepatic metastasis induced by human colorectal cancer cell line, HT29 (21). More recently, several human mAbs against IGF-II have been reported (11, 16) and IGF-I and an IGF-II cross-reactive mAb is also described (22). These results suggest that binding to IGF-I and IGF-II can markedly affect tumor growth and that mAbs against the 2 ligands are promising candidate therapeutics.

Here, we describe the identification and characterization of a human mAb (m708.5) which bound with high affinity to IGF-I ($K_D = 200$ pmol/L) and IGF-II ($K_D = 60$ pmol/L). It potently inhibited signal transduction mediated by the IGF1R interaction with IGF-I and IGF-II and the interaction of the IR with IGF-II, resulting in the inhibition of phosphorylation of IGF1R, IR, and cancer cell growth. These results suggest that m708.5 may have potential as a candidate therapeutic.

Materials and Methods

Panning of a large phage displayed Fab library

Recombinant human IGF-I was used to pan a human naive Fab phage library containing 10^{10} unique clones as previously described (23).

Mutagenesis by error-prone PCR

Error-prone PCR of the entire scFv gene was carried out using Stratagene GeneMorph II Random Mutagenesis Kit according to the instructions of the manufacturer. Briefly, PCR was done in a 50-μL reaction containing 1× Mutazyme II reaction buffer, 0.5 μmol/L each of primers: ERRORF (5′-GATATATCCATGGCCCAGGCGGCC-3′) and ERRORR (5′-ACCACTAGTTGGGCCGGCCTG-3′), 0.2 mmol/L (each) dNTPs, 1 ng of DNA template, 2 μmol/L 8-oxo-deoxyguanosine triphosphate, 2 μmol/L 2′-deoxy-*p*-nucleoside-5′-triphosphate, and 2.5 U of Mutazyme II DNA polymerase. The reaction mixtures were denatured at 95°C for 2 minutes, cycled 35 times at 95°C for 1 minute, 60°C for 1 minute, and 72°C for 1 minute and finally extended at 72°C for 10 minutes. The PCR products were gel purified and amplified in 4 100-μL PCR reactions containing 1× Accuprime PCR reaction mix (Invitrogen), 1 μmol/L of primers YDRDF (5′-CTTCGCTGTTTTTCAATATTTTCTGTTATTGCTTCAGTTTTGGCCCAGGCGGCC-3′) and YDRDR (5′-GAGCCGCCACCCTCAGAACCGCCACCCTCAGAGCCACCACTAGTTGGGCCGGCCTG-3′), 120 ng of error-prone PCR product, and 2.5 U of Accuprime pfx DNA polymerase (Invitrogen). The reactions were thermally cycled using the same conditions except that 30 cycles were used. Amplified insert was gel purified and concentrated using vacuum concentrator.

Construction of yeast displayed mutant libraries

The yeast display vector used for library construction, pYD7, was modified from pCTCON2 (24). Two *Sfi*I restriction sites of pYD7 before and after the scFv matched the cloning sites of the phage display vector. This allowed fragments to be conveniently shuttled between the yeast vector and phage display vector. Furthermore, to better present displayed antibodies on yeast surface, scFvs were fused at the N-terminal of the yeast protein agglutinin (Aga2p).

The pYD7 vector was digested with *Sfi*I and gel purified. Multiple aliquots of 12 μg of mutagenized scFv DNA and 4 μg of plasmid DNA were concentrated into 20 to 30 μL of water. The pYD7-scFv libraries were then electroporated into competent yeast cells EBY100 prepared as described previously (25). Briefly, 10 mL of EBY100 yeast cells in YPD media (10 g/L yeast nitrogen base, 20 g/L peptone, and 20 g/L glucose) were grown at 30°C with shaking at 250 rpm overnight. The culture was inoculated into 100 mL of fresh YPD and allowed to grow to OD_{600} of 1.6 before collecting by centrifugation. The cell pellet was washed twice with 50 mL of cold water and once with 50 mL cold electroporation buffer (1 mol/L sorbitol, 1 mmol/L $CaCl_2$). Cells were conditioned in 20 mL of incubation buffer (0.1 mol/L LiAc, 10 mmol/L DTT) at 30°C with shaking at 250 rpm for 30 minutes. Cells were washed 1 more time with 50 mL of electroporation buffer, then resuspended in the same buffer to reach 1 mL volume. Each electroporation mixture included 400 μL of yeast cell suspension, 4 μg linearized vector, and 12 μg insert DNA. Cells were electroporated at 2.5 kV and 25 μF in BioRad GenePulser cuvettes (0.2-cm electrode gap). After electroporation, cells were resuspended in 20 mL of 1:1 (v:v) mix of 1 mol/L sorbitol:YPD media and incubated at 30°C for 1 hour. Finally, the cells were collected and amplified in SDCAA media (20 g/L glucose, 6.7 g/L yeast nitrogen base without amino acids, 5.4 g/L Na_2HPO_4, 8.6 g/L $NaH_2PO_4.H_2O$, and 5 g/L casamino acids) at 30°C with shaking at 250 rpm for 24 to 48 hours.

Selection of binders from the yeast libraries

Typically, amplified yeast library was transferred to SG/RCAA media (20 g/L galactose, 20 g/L raffinose, 1 g/L glucose, 6.7 g/L yeast nitrogen base without amino acids, 5.4 g/L Na_2HPO_4, 8.6 g/L $NaH_2PO_4.H_2O$, and 5 g/L casamino acids) for induction at 20°C for 16 to 18 hours in culture density and volume appropriate for the size of the library.

The methodology for generating and isolating higher affinity mutants was as described in references (24, 26, 27). Antigen concentrations are chosen based on the equilibrium dissociation constant (K_D) of the parental antibody. The antigen incubation volume must be large enough to allow at least 10-fold excess of the antigen over amounts of scFv displayed on yeast (assuming 5×10^4 scFv per yeast cell; ref. 24). Antigen incubation times were chosen to ensure that the reaction reached at least 90% of

equilibrium calculated as described in reference (28). Before fluorescence-activated cell sorting (FACS), induced yeast library (1×10^9) was incubated with 10 μg IGF-I-conjugated magnetic beads for 1 hour at room temperature in PBSA buffer (0.1% bovine serum albumin in PBS), followed by separation with a magnetic stand. The isolated yeast cells were washed 3 times with PBSA buffer and added into 10 mL of SDCAA media for amplification overnight in a 30°C shaker with 250 rpm. The amplified yeast cells were induced in SG/RCAA media for 18 hours at 20°C with 250 rpm shaking. For the first FACS selection of the first round, approximately 1×10^8 yeast cells were pelleted, washed twice with PBSA buffer, and resuspended in 1 mL PBSA buffer with 3 nmol/L biotinylated IGF-I and 2 μg/mL of mouse anti-c-myc antibody (Invitrogen). After incubation, yeast cells were washed 3 times and then resuspended in 1 mL PBSA buffer. Both 1:50 diluted R-phycoerythrin–conjugated streptavidin (Invitrogen) and Alexa Fluor 488–conjugated goat anti-mouse IgG antibody (Invitrogen) were added to yeast cells. Cells were incubated at 4°C for 30 minutes and washed 3 times with PBSA buffer and then resuspended in PBSA buffer for sorting. Sorting gates were determined to select only the population with higher antigen-binding signals. Collected cells were grown overnight in SDCAA media at 30°C and induced in SG/RCAA for the next sorting. For the next 2 FACS selections, approximately 1×10^7 to 2×10^7 yeast cells were used for staining with 1 and 0.3 nmol/L biotinylated IGF-I, respectively.

Two and 3 FACS selections were carried out in second and third round. Yeast cells were pelleted, washed in PBSA buffer, resuspended in PBSA buffer with biotinylated IGF-I (ranging from 3 to 0.1 nmol/L) and mouse anti-c-myc antibody, and incubated on ice. Cells were then washed with PBSA twice and resuspended in 1 mL PBSA with R-phycoerythrin–conjugated streptavidin and Alexa Fluor 488–conjugated goat anti-mouse antibody.

After the first and second round, yeast plasmids were isolated using Zymoprep Yeast Plasmid Miniprep II Kit (Zymo Research) according to the manufacturer's instructions and used as templates for error-prone PCR to amplify gene repertoire for the construction of the second and third mutant libraries. Cells from the last selection of the third round were spread on SDCAA plates. Monoclonal yeast cells were characterized, and isolated antibodies with improved affinity were sequenced.

Conversion to IgG1 and expression of Fab, scFv, and IgG1

We used the same procedure as previously described (29). Fab and scFv were expressed and purified as previously described (30, 31).

ELISA binding assay

Antigens (50 ng) per well were coated on 96-well ELISA plates overnight at 4°C. For phage ELISA, approximately 1×10^{10} plaque-forming unit phages were incubated with antigen for 1 hour. Bound phages were detected with anti-M13-HRP mAb (1:3,000; GE Healthcare). For Fab and IgG1 ELISA, Fabs and IgG1s with different dilutions were incubated with antigens for 1 hour. Bound Fabs were detected with anti-FLAG-HRP mAb (1:3,000; Sigma). Bound IgG1s were detected with anti-human Fc-HRP mAb (1:2,000; Invitrogen). The 2,2′-azino-bis-(3-ethylbenzthiazoline-6-sulfonic acid) substrate (Sigma) was added and the reaction was read at 450 nm.

Affinity measurement of yeast-displayed scFvs

The equilibrium dissociation constant was determined essentially as previously described (32).

Affinity determination by surface plasmon resonance

Interactions between various isolated antibodies and IGF-I and IGF-II were analyzed by surface plasmon resonance technology using a Biacore X100 instrument (GE healthcare). IGF-I or IGF-II was covalently immobilized onto a sensor chip (CM5) using carbodiimide coupling chemistry. A control reference surface was prepared for nonspecific binding and refractive index changes. For analysis of the kinetics of interactions, varying concentrations of antibodies were injected at flow rate of 30 μL/min using running buffer containing 10 mmol/L HEPES, 150 mmol/L NaCl, 3 mmol/L EDTA, and 0.05% Surfactant P-20 (pH = 7.4). The association and dissociation phase data were fitted simultaneously to a 1:1 model by using BIAevaluation 3.2. All the experiments were done at 25°C.

Competition assay

scFv or IgG1 m708.5 (10 nmol/L) was incubated with 5 nmol/L biotinylated human IGF-I and 1 nmol/L biotinylated human IGF-II at room temperature for 20 minutes. The mixtures were added to 5×10^5 MCF-7 cells in 50 μL PBSA buffer and incubated for 30 minutes on ice. After washing once, cells were incubated with a 1:50 dilution of R-phycoerythrin–conjugated streptavidin for 30 minutes on ice, then washed again, and resuspended in 0.5 mL PBSA buffer. Analysis was conducted using a BD Bioscience FACScalibur. Irrelevant anti-gp41 MPER scFv-3A2a (unpublished data) and anti-Nipah/Hendra viruses IgG1-m102.4 (33) were used as negative controls.

Phosphorylation assay

Measurement of IGF1R and IR phosphorylation was conducted as previously described (11) except that the treatment medium was made by adding 1 nmol/L human IGF-I or 5 nmol/L human IGF-II.

Cell growth assay

Cell growth and inhibition were measured as previously described (11) except that IGF-I (2.5 nmol/L) was also used in addition to IGF-II (2.5 nmol/L).

Results

Identification of a high affinity IGF-I and IGF-II cross-reactive human mAb, m708.2

To develop human mAbs against human IGF-I, we used a large size ($\sim 10^{10}$ independent clones) naive human Fab phage–displayed library. A recombinant human IGF-I was conjugated to magnetic beads and used as the antigen for pannings. After 3 rounds of panning, more than 200 random individual phage clones were screened by phage ELISA against IGF-I. Clones that exhibited significant binding to IGF-I were sequenced. Finally, 3 clones with unique sequences were found. They were expressed in bacteria as soluble Fabs, purified, and tested for binding activity in ELISA. Two Fabs, designated m705 and m706, showed binding specifically to IGF-I only, whereas 1 Fab, m708, bound to both IGF-I and IGF-II in ELISA (Supplementary Fig. S1). m708 was selected for affinity maturation by light chain shuffling.

Two rounds of panning of the light chain shuffled library (containing 2×10^8 independent clones) against IGF-I-conjugated magnetic beads were conducted, and 200 clones from the second round of panning were screened by phage ELISA. Among them, Fab m708.2 showed markedly higher binding to both IGF-I and IGF-II than the parental m708 version (data not shown) and was selected for further improvement.

Construction of m708.2 mutant libraries displayed on yeast and selection of a picomolar affinity binder, m708.5

To further increase the affinity of m708.2, it was converted to a scFv and randomly mutagenized by error-prone PCR. We used yeast display for further maturation, because it allows fine discrimination between mutants by flow cytometry and our attempts to increase affinity by phage display were not successful. Therefore, the mutant library was displayed on yeast cells by homologous recombination with a vector containing a C-terminal Aga2 protein and c-myc tag. To obtain large amounts of DNA insert and avoid improper incorporation at the site of homologous recombination, purified DNA obtained from the first PCR reaction was reamplified in a second PCR reaction. Thus, 30% to 40% of the transformed cells displayed scFvs as verified by flow cytometry (data not shown).

Mutant yeast library of relatively large (up to 10^9) size was generated and subjected first to 1 round of selection by using IGF-I-conjugated magnetic beads according to the method described in references (34, 35). This allowed elimination of yeast cells that did not express antibodies or bound weakly to IGF-I. The library was then sorted several times by FACS for binding to IGF-I. The sorted scFvs were mutated by error-prone PCR of the entire gene to yield a new sublibrary. The process of sorting and mutagenesis was then cyclically repeated (Fig. 1). The highest affinity clones from the final round of maturation were identified (Fig. 2) and their sequences were analyzed.

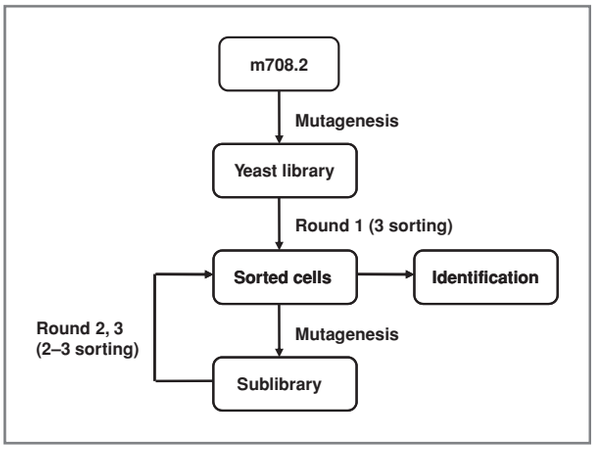

Figure 1. Affinity maturation scheme.

One dominant clone, m708.5, was identified by sequence analysis. Compared with m708.2, m708.5 had 2 amino acid substitutions in the heavy chain CDR2 (H2), 2 amino acid substitutions in H3, and 9 amino acid substitutions in the framework region (Table 1). There were 4 substitutions in the framework regions of the light chain. These substitutions resulted in a remarkable improvement of affinity but still retaining cross-reactivity as measured by 2 different methods. The first method was based on yeast-displayed scFvs that were incubated with varying concentrations of biotinylated IGF-I or IGF-II. The affinity of yeast-displayed m708.5 scFv for IGF-I was increased 39-fold compared with that of m708.2 (1×10^{-10} vs. 3.9×10^{-9} mol/L), whereas its affinity for IGF-II was increased 27-fold (4.1×10^{-11} vs. 1.1×10^{-9} mol/L; Table 2). Similar values were obtained for isolated soluble scFv m708.5 as measured with surface plasmon resonance (Supplementary Fig. S2): 2×10^{-10} mol/L for IGF-I and 6.1×10^{-11} mol/L for IGF-II, compared with scFv m708.2 (2.2×10^{-9} mol/L for IGF-I and 1.8×10^{-9} mol/L for IGF-II; Table 2). Therefore, the cross-reactive antibody m708.2 was successfully matured to a scFv, m708.5, with picomolar affinity for both IGF-I and IGF-II.

Avidity of IgG1 m708.5

The scFv m708.5 was converted to an IgG1 format and its avidity measured with surface plasmon resonance. IgG1 m708.5 showed increased binding for both IGF-I and IGF-II compared with scFv m708.5. The effective K_D of m708.5 for IGF-I and IGF-II was 1,000-fold and 60-fold higher than K_D for scFv, respectively (data not shown). The measured K_D ($<10^{-12}$ mol/L) is below the sensitivity of the Biacore instrument [10^6 $(\text{mol/L})^{-1}\text{s}^{-1}$ for k_{on} and 10^{-6} s^{-1} for k_{off}] and therefore may not be reliable. IgG1 m708.5 was also much more effective in binding to both IGF-I and IGF-II than m708.2 as measured by ELISA (Fig. 3). Thus, m708.5 exhibited very high avidity in IgG1 format, resulting in much stronger binding than in scFv format.

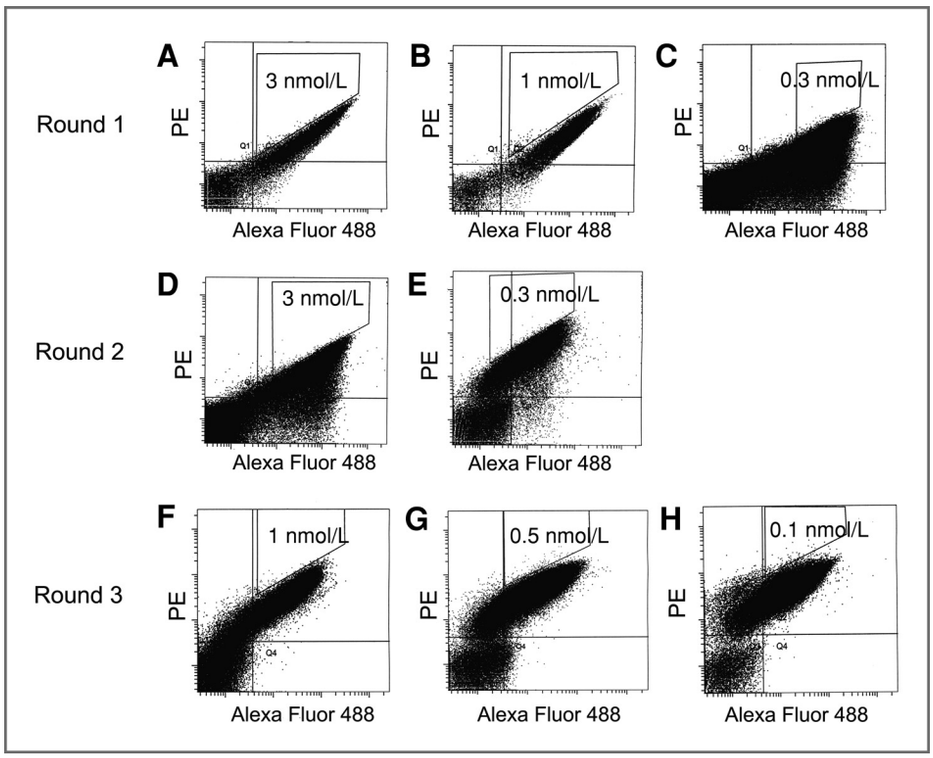

Figure 2. FACS for affinity maturation. Yeast libraries were labeled with mouse anti-c-myc antibody followed by Alexa Fluor 488-conjugated goat antimouse antibody as well as biotinylated IGFI-I followed by R-phycoerythrin-conjugated streptavidin. A–C, during 3 FACS selections of round 1, yeast cells were stained with concentrations of biotinylated IGF-I at 3, 1, and 0.3 nmol/L, respectively. D and E, during 2 FACS selections of round 2, yeast cells were stained with concentrations of biotinylated IGF-I at 3 and 0.3 nmol/L, respectively. F–H, during 3 FACS selections of round 3, yeast cells were stained with concentrations of biotinylated IGF-I at 1, 0.5, and 0.1 nmol/L. The 0.1% to 0.3% cells were selected from sort gates. PE, phycoerythrin.

m708.5 inhibits binding of IGF-I and IGF-II to IGF1R and IR and their phosphorylation

IGFs bind and activate IGF1R and the signals transduced by this pathway lead to cell proliferation. To find whether m708.5 inhibits binding of IGF-I and IGF-II to IGF1R and IR, we used the breast cancer cell line MCF-7, which has been shown to express both receptors. m708.5 in scFv and IgG1 completely blocked IGF-I and IGF-II binding to their receptors on MCF-7 cells (Fig. 4). Control scFv and IgG that did not recognize IGFs had no effect. The antibody also inhibited IGF-I-induced (1 nmol/L) or IGF-II-induced (5 nmol/L) phosphorylation. Immunoblottings (Fig. 5A) showed that from 1 to 100 nmol/L, m708.5 completely inhibited the IGF-I-induced phosphorylation of IGF1R. Similar inhibitory activity was also observed with m708.2, which however only partly blocked IGF-I-induced phosphorylation at 10 nmol/L. In addition to IGF-I, both m708.2 and m708.5, as well as m610 were capable of inhibiting IGF-II-induced phosphorylation of IGF1R (Fig. 5B). However, m708.5 was superior to m708.2 (Fig. 5B) and competed with m610. The antibodies also inhibited IGF-II-mediated phosphorylation of the IR induced by 5 nmol/L of IGF-II (Fig. 5C). The inhibition was independent on human insulin that m708.5 did not bind (Fig. 5D). Therefore, m708.5 could effectively inhibit ligand-induced phosphorylation of the 2 receptors without inhibiting insulin–IR interaction.

Inhibition of MCF-7 cell growth by m708.5

To investigate whether the blocking of IGF binding by m708.5 is potent enough to inhibit the proliferation of cells, we tested the activity of m708.5 in a cell growth

Table 1. Sequences of the m708.2 and m708.5 heavy chain CDRs

Clone	H1[a]	H2[b]	H3[c]
m708.2	G G T F S S Y A	I I P I L G I A	A R G P R G Y S Y N F D Y
m708.5	- - - - - - - - - - -	- - - T - - V	- G - - - - - - - - - - N

Identical residues are denoted by:
[a]H1 is CDR1 of heavy chain;
[b]H2 is CDR2 of heavy chain;
[c]H3 is CDR3 of heavy chain.

Table 2. Binding rate constants and affinities of scFv m708.2 and m708.5, as measured by FACS and Biacore

Antibody	Antigen	FACS,[a] K_D, mol/L	Biacore[b]		
			k_{on}, $(mol/L)^{-1}s^{-1}$	k_{off}, s^{-1}	K_D, mol/L
m708.2 scFv	IGF1	3.9×10^{-9}	1.1×10^{6}	2.4×10^{-3}	2.2×10^{-9}
	IGF2	1.1×10^{-9}	2.3×10^{5}	4.0×10^{-4}	1.8×10^{-9}
m708.5 scFv	IGF1	1.0×10^{-10}	1.4×10^{6}	2.8×10^{-4}	2.0×10^{-10}
	IGF2	4.1×10^{-11}	4.1×10^{6}	2.5×10^{-6}	6.1×10^{-11}

[a]Values for yeast-displayed scFvs.
[b]Values for purified soluble scFvs.

assay using MCF-7 cells. After 3 days of treatment, the cell growth was almost completely inhibited at 320 nmol/L of m708.5 (Fig. 6). At concentrations higher than 40 nmol/L, m708.5 treatment resulted in more than 40% cell growth inhibition. In contrast, m708.2 could only inhibit cancer cells at concentrations higher than 80 nmol/L and 40% inhibition was achieved above 160 nmol/L. It is noteworthy that MCF-7 cells produced significant amounts of IGF-II concentrations of up to 35 nmol/L after 3 days (11). These data showed that the potency of m708.5 was remarkably improved compared with m708.2, and it effectively inhibited tumor cell proliferation *in vitro*.

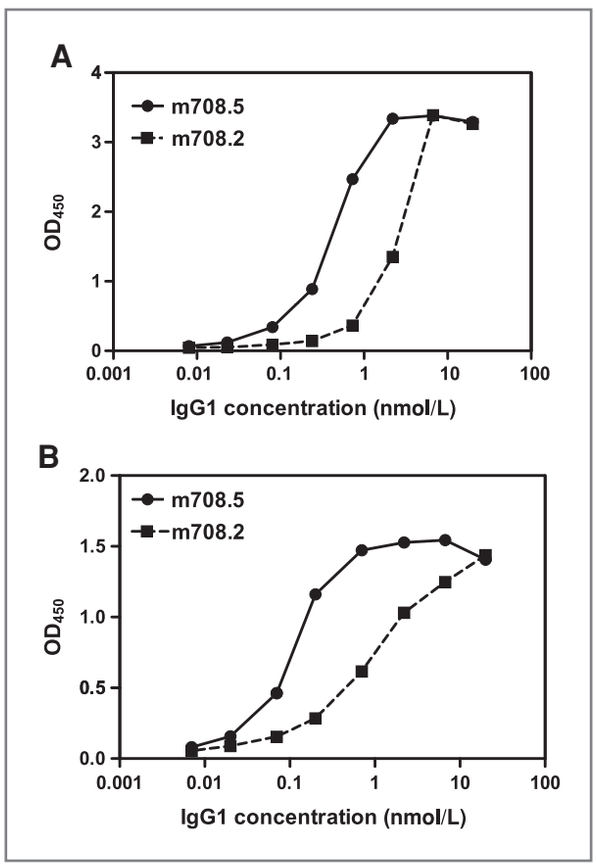

Figure 3. Binding of IgG1 m708.2 and m708.5 to IGF-I and IGF-II. IgG1 m708.2 and m708.5 were serially diluted and added to wells coated with IGF-I (A) or IGF-II (B). Bound IgG1 was detected with a horseradish peroxidase-conjugated anti-human Fc antibody and measured as optical densities (OD) at 450 nm. The data are representative of 3 separate experiments carried out in duplicates with variations not exceeding 10%.

Discussion

The IGF signaling system plays an important role in tumorigenesis (36). Human IGF-I and IGF-II share 62% sequence identity and have overlapping functions: both IGF-I and IGF-II can activate the IGF1R that can drive tumor cell proliferation. A remarkable feature of IGF-II (but not IGF-I) is that it can also bind to the IR and enhance cell proliferation. To further explore novel cancer therapeutics based on human mAbs targeting components of the IGF system, we identified 3 human antibodies specific for IGF-I using phage display technologies. One of them, m708, exhibited also significant binding to human IGF-II and was further affinity matured by light chain shuffling, mutagenesis, and yeast display. The affinity-maturated antibody, m708.5, potently inhibited both IGF-I- and IGF-II-induced phosphorylation of IGF1R as well as IGF-II-induced phosphorylation of the IR and less potently growth of MCF-7 cancer cell–expressing IGF1R.

The inhibitory activity of the antibodies was cell type dependent (data not shown) with a likely major determinant being the surface concentration of the IGF1R and the IR. To date, many IGF1R-specific antibodies have been under preclinical studies and several are being evaluated in clinical trials (1). We previously reported a human mAb (m610) with high affinity to IGF-II that potently blocked the growth/migration of human cancer lines *in vitro* (11) and significantly suppressed the growth of prostate cancer cells in a human bone environment (37). A murine mAb cross-reactive to human IGF-I and IGF-II inhibited the development of new bone tumors and the progression of established tumors (20). Recently, a new mAb against IGF-I and IGF-II was reported that was effective in a mouse model of caner with cells expressing high levels of IGF1R (22). On the

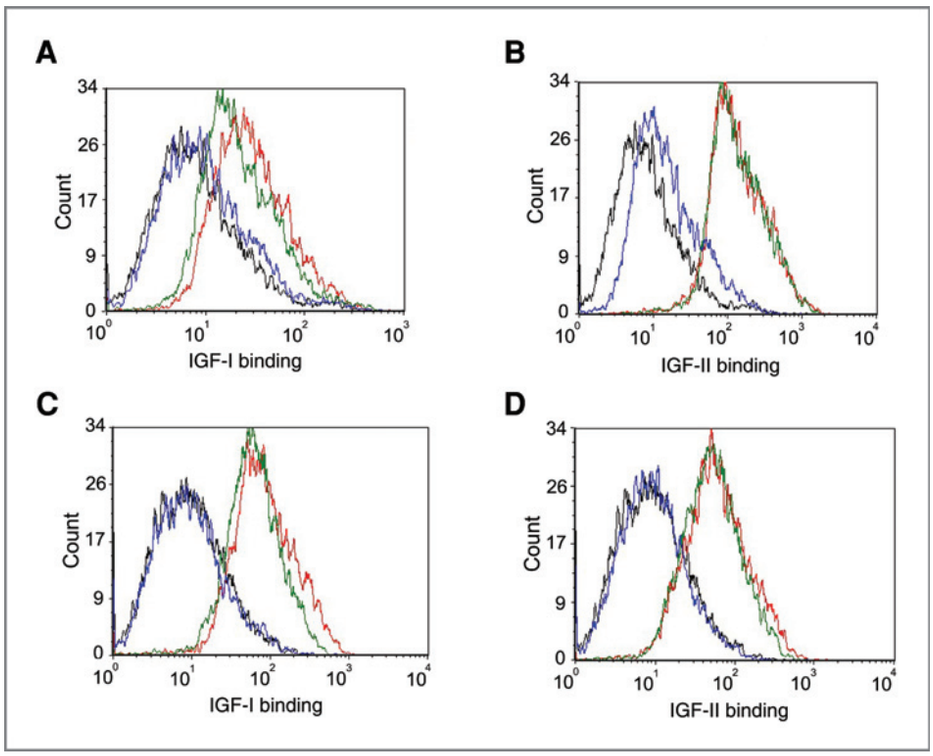

Figure 4. Inhibition of IGF-I and IGF-II binding to MCF-7 cells by m708.5. A and B, scFv m708.5 scFv and control scFv 3A2a were preincubated with biotinylated IGF-I (A) and biotinylated IGF-II (B) for 20 minutes at room temperature. Then, mixtures were incubated with MCF-7 cells for 30 minutes on ice. C and D, IgG1 m708.5 and control IgG1 m102.4 were preincubated with biotinylated IGF-I (C) and biotinylated IGF-II (D) for 20 minutes at room temperature. Then, mixtures were incubated with MCF-7 cells for 30 minutes on ice. After the staining of R-phycoerythrin–conjugated streptavidin for 30 minutes on ice, cells were detected by flow cytometry. In all the graphs, black lines are for cells without any antibody labeling. Blue lines are for tested antibodies, and green lines are for the control antibodies. Red lines show binding with IGF-I or IGF-II alone. Data shown are representative of 3 separate experiments carried out in duplicates with similar results.

basis of the data described in our article and those previously reported, we believe that m708.5 would also exhibit inhibitory activity *in vivo*. The finding that IgG1 m708.5 also binds IGF-I and IGF-II is important, because it would allow the use of the IgG antibody format, which is most stable and has long half-life *in vivo*.

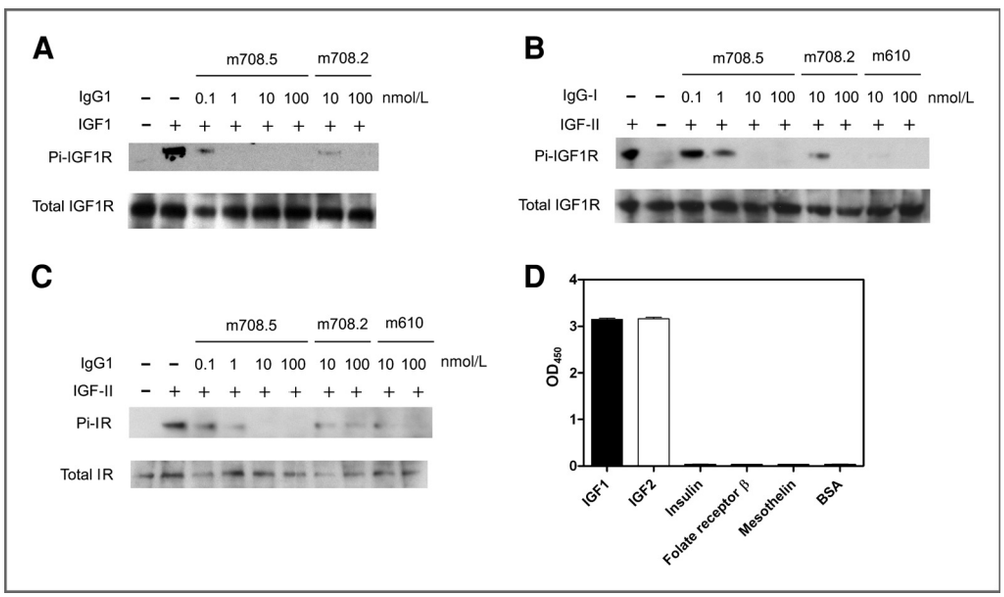

Figure 5. Inhibition of IGF1R and IR phosphorylation by m708.2 and m708.5 and absence of m708.5 binding to human insulin. A and B, MCF-7 cells were starved in serum-free medium for 5 hours first, followed by addition of treatment medium with 1 nmol/L IGF-I (A) or 5 nmol/L IGF-II (B) with indicated concentrations of IgG1s. Thirty minutes later, cells were chilled and lysed. IGF1R was immunoprecipitated, and the phosphorylated IGF1R was detected with a phosphotyrosine–specific antibody. The total amount of IGF1R was detected by the same polyclonal antibody used for the immunoprecipitation. C, MCF-7 cells were starved and treated with 5 nmol/L IGF-II with indicated concentrations of IgG1s. The phosphorylated IR was detected with a phosphotyrosine–specific antibody. The total amount of IR was detected. D, IgG1 m708.5 (10 nmol/L) was added to wells coated with IGF-I and IGF-II, human insulin, and irrelevant antigens. Bound IgG1 was detected with a horseradish peroxidase-conjugated anti-human Fc antibody and measured as optical densities (OD) at 450 nm. Data shown are representative of 3 separate experiments carried out in duplicates with similar results. BSA, bovine serum albumin.

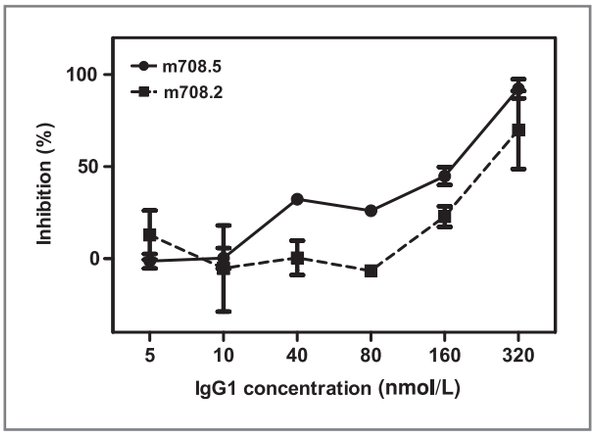

Figure 6. Growth inhibition of MCF-7 cells by m708.2 and m708.5. MCF-7 cells were incubated in complete medium overnight. Different concentrations of IgG1 m708.2 and m708.5 were preincubated with added IGF-I (2.5 nmol/L) and IGF-II (2.5 nmol/L) for 15 minutes. The media of MCF-7 cells were replaced by the mixture of IgG1 and ligands immediately. Cells were allowed to grow for 3 days, and MTS substrate was added to detect viable cells. The reaction was monitored by absorbance at 450 nm. Positive control were cells in serum-free medium with IGF ligands. Blank control was cells in serum-free medium without any IGFs. Shown are data with mean ± SEM calculated from 3 separate experiments.

m708.5 is a fully human mAb cross-reactive to both human IGF-I and IGF-II with picomolar affinity and potently inhibits signal transduction mediated by IGF-I and IGF-II interacting with IGF1R and IGF-II interacting with IR. It also inhibits potently tumor cell growth *in vitro* and is likely to exert similar activity *in vivo*. Importantly, m708.5 cross-reacts to mouse IGF-I and IGF-II (Supplementary Fig. S3). Therefore, the activity of m708.5 can be tested with human xenografts in mouse models of cancer where it could inhibit both autocrine (human) and paracrine (mouse) IGF. Therefore, m708.5 offers a new and promising therapeutic strategy for treating tumor cells and a possible therapeutic addition to IGF1R-targeted agents. It could be used in combination with other IGF-I and IGF-II- or IGF1R-targeting mAbs and also with other cancer therapeutics. We do not know where exactly its epitope is located, although it inhibits binding of IGF-I and IGF-II to both IGF1R and IR, and therefore, its epitope may overlap with their binding sites although steric hindrance is also possible. It competes with our previously identified anti-IGF-II mAb m610 for binding to IGF-II, and therefore, their epitopes are likely to be overlapped although steric hindrance could not be excluded. It would be interesting to find out whether m708.5 competes with the recently described mAbs against IGF-I and IGF-II. Further research is needed to exactly localize the epitope of m708.5 and evaluate its inhibitory properties *in vivo* as a candidate therapeutic.

Disclosure of Potential Conflicts of Interest

No potential conflicts of interest were disclosed.

Acknowledgments

The authors thank Dr. Dane Wittrup for providing reagents and members of our group for helpful discussions.

Grant Support

This research was supported by the Intramural Research Program of the NIH, National Cancer Institute, Center for Cancer Research.

The costs of publication of this article were defrayed in part by the payment of page charges. This article must therefore be hereby marked *advertisement* in accordance with 18 U.S.C. Section 1734 solely to indicate this fact.

Received April 15, 2011; revised June 7, 2011; accepted June 27, 2011; published OnlineFirst July 12, 2011.

References

1. Pollak M. Insulin and insulin-like growth factor signalling in neoplasia. Nat Rev Cancer 2008;8:915–28.
2. Yee D. Targeting insulin-like growth factor pathways. Br J Cancer 2007;96 Suppl:R7–10.
3. Foulstone E, Prince S, Zaccheo O, Burns JL, Harper J, Jacobs C, et al. Insulin-like growth factor ligands, receptors, and binding proteins in cancer. J Pathol 2005;205:145–53.
4. Samani AA, Yakar S, LeRoith D, Brodt P. The role of the IGF system in cancer growth and metastasis: overview and recent insights. Endocr Rev 2007;28:20–47.
5. Wang Y, Sun Y. Insulin-like growth factor receptor-1 as an anti-cancer target: blocking transformation and inducing apoptosis. Curr Cancer Drug Targets 2002;2:191–207.
6. Hofmann F, Garcia-Echeverria C. Blocking the insulin-like growth factor-I receptor as a strategy for targeting cancer. Drug Discov Today 2005;10:1041–7.
7. Smith TJ. Insulin-like growth factor-I regulation of immune function: a potential therapeutic target in autoimmune diseases? Pharmacol Rev 2010;62:199–236.
8. Hernandez-Sanchez C, Blakesley V, Kalebic T, Helman L, LeRoith D. The role of the tyrosine kinase domain of the insulin-like growth factor-I receptor in intracellular signaling, cellular proliferation, and tumorigenesis. J Biol Chem 1995;270:29176–81.
9. Feng Y, Dimitrov DS. Monoclonal antibodies against components of the IGF system for cancer treatment. Curr Opin Drug Discov Devel 2008;11:178–85.
10. Zha J, O'Brien C, Savage H, Huw LY, Zhong F, Berry L, et al. Molecular predictors of response to a humanized anti-insulin-like growth factor-I receptor monoclonal antibody in breast and colorectal cancer. Mol Cancer Ther 2009;8:2110–21.
11. Feng Y, Zhu Z, Xiao X, Choudhry V, Barrett JC, Dimitrov DS. Novel human monoclonal antibodies to insulin-like growth factor (IGF)-II that potently inhibit the IGF receptor type I signal transduction function. Mol Cancer Ther 2006;5:114–20.
12. Resnicoff M, Coppola D, Sell C, Rubin R, Ferrone S, Baserga R. Growth inhibition of human melanoma cells in nude mice by antisense strategies to the type 1 insulin-like growth factor receptor. Cancer Res 1994;54:4848–50.
13. Wang Y, Lipari P, Wang X, Hailey J, Liang L, Ramos R, et al. A fully human insulin-like growth factor-I receptor antibody SCH 717454 (Robatumumab) has antitumor activity as a single agent and in combination with cytotoxics in pediatric tumor xenografts. Mol Cancer Ther 2010;9:410–8.
14. Zhang MY, Feng Y, Wang Y, Dimitrov DS. Characterization of a chimeric monoclonal antibody against the insulin-like growth factor-I receptor. MAbs 2009;1:475–80.

15. Su JL, Stimpson S, Edwards C, Van Arnold J, Burgess S, Lin P. Neutralizing IGF-1 monoclonal antibody with cross-species reactivity. Hybridoma 1997;16:513–8.
16. Dransfield DT, Cohen EH, Chang Q, Sparrow LG, Bentley JD, Dolezal O, et al. A human monoclonal antibody against insulin-like growth factor-II blocks the growth of human hepatocellular carcinoma cell lines *in vitro* and *in vivo*. Mol Cancer Ther 2010;9:1809–19.
17. Rodon J, DeSantos V, Ferry RJ Jr, Kurzrock R. Early drug development of inhibitors of the insulin-like growth factor-I receptor pathway: lessons from the first clinical trials. Mol Cancer Ther 2008;7:2575–88.
18. Tolcher AW, Sarantopoulos J, Patnaik A, Papadopoulos K, Lin CC, Rodon J, et al. Phase I, pharmacokinetic, and pharmacodynamic study of AMG 479, a fully human monoclonal antibody to insulin-like growth factor receptor 1. J Clin Oncol 2009;27:5800–7.
19. Kurmasheva RT, Dudkin L, Billups C, Debelenko LV, Morton CL, Houghton PJ. The insulin-like growth factor-1 receptor-targeting antibody, CP-751,871, suppresses tumor-derived VEGF and synergizes with rapamycin in models of childhood sarcoma. Cancer Res 2009;69:7662–71.
20. Goya M, Miyamoto S, Nagai K, Ohki Y, Nakamura K, Shitara K, et al. Growth inhibition of human prostate cancer cells in human adult bone implanted into nonobese diabetic/severe combined immunodeficient mice by a ligand-specific antibody to human insulin-like growth factors. Cancer Res 2004;64:6252–8.
21. Miyamoto S, Nakamura M, Shitara K, Nakamura K, Ohki Y, Ishii G, et al. Blockade of paracrine supply of insulin-like growth factors using neutralizing antibodies suppresses the liver metastasis of human colorectal cancers. Clin Cancer Res 2005;11:3494–502.
22. Gao J, Chesebrough JW, Cartlidge SA, Ricketts SA, Incognito L, Veldman-Jones M, et al. Dual IGF-I/II-neutralizing antibody MEDI-573 potently inhibits IGF signaling and tumor growth. Cancer Res 2011; 71:1029–40.
23. Zhu Z, Dimitrov DS. Construction of a large naive human phage-displayed Fab library through one-step cloning. Methods Mol Biol 2009;525:129–42, xv.
24. Chao G, Lau WL, Hackel BJ, Sazinsky SL, Lippow SM, Wittrup KD. Isolating and engineering human antibodies using yeast surface display. Nat Protoc 2006;1:755–68.
25. Benatuil L, Perez JM, Belk J, Hsieh CM. An improved yeast transformation method for the generation of very large human antibody libraries. Protein Eng Des Sel 2010;23:155–9.
26. Boder ET, Midelfort KS, Wittrup KD. Directed evolution of antibody fragments with monovalent femtomolar antigen-binding affinity. Proc Natl Acad Sci U S A 2000;97:10701–5.
27. Boder ET, Wittrup KD. Yeast surface display for directed evolution of protein expression, affinity, and stability. Methods Enzymol 2000; 328:430–44.
28. Garcia-Rodriguez C, Levy R, Arndt JW, Forsyth CM, Razai A, Lou J, et al. Molecular evolution of antibody cross-reactivity for two subtypes of type A botulinum neurotoxin. Nat Biotechnol 2007;25:107–16.
29. Feng Y, Xiao X, Zhu Z, Streaker E, Ho M, Pastan I, et al. A novel human monoclonal antibody that binds with high affinity to mesothelin-expressing cells and kills them by antibody-dependent cell-mediated cytotoxicity. Mol Cancer Ther 2009;8:1113–8.
30. Zhu Z, Chakraborti S, He Y, Roberts A, Sheahan T, Xiao X, et al. Potent cross-reactive neutralization of SARS coronavirus isolates by human monoclonal antibodies. Proc Natl Acad Sci U S A 2007;104:12123–8.
31. Zhao Q, Chan YW, Lee SS, Cheung WT. One-step expression and purification of single-chain variable antibody fragment using an improved hexahistidine tag phagemid vector. Protein Expr Purif 2009; 68:190–5.
32. Hackel BJ, Kapila A, Wittrup KD. Picomolar affinity fibronectin domains engineered utilizing loop length diversity, recursive mutagenesis, and loop shuffling. J Mol Biol 2008;381:1238–52.
33. Zhu Z, Bossart KN, Bishop KA, Crameri G, Dimitrov AS, McEachern JA, et al. Exceptionally potent cross-reactive neutralization of Nipah and Hendra viruses by a human monoclonal antibody. J Infect Dis 2008;197:846–53.
34. Blaise L, Wehnert A, Steukers MP, van den Beucken T, Hoogenboom HR, Hufton SE. Construction and diversification of yeast cell surface displayed libraries by yeast mating: application to the affinity maturation of Fab antibody fragments. Gene 2004;342:211–8.
35. Yeung YA, Wittrup KD. Quantitative screening of yeast surface-displayed polypeptide libraries by magnetic bead capture. Biotechnol Prog 2002;18:212–20.
36. LeRoith D, Roberts CT Jr. The insulin-like growth factor system and cancer. Cancer Lett 2003;195:127–37.
37. Kimura T, Kuwata T, Ashimine S, Yamazaki M, Yamauchi C, Nagai K, et al. Targeting of bone-derived insulin-like growth factor-II by a human neutralizing antibody suppresses the growth of prostate cancer cells in a human bone environment. Clin Cancer Res 2010;16: 121–9.